Available online at www.sciencedirect.com

ScienceDirect

Mendeleev Commun., 2020, **30**, 192–194

Mendeleev Communications

Carbon dioxide reduction under visible light: a comparison of cadmium sulfide and titania photocatalysts

Mikhail N. Lyulyukin, Anna Y. Kurenkova, Andrey V. Bukhtiyarov and Ekaterina A. Kozlova*

G. K. Boreskov Institute of Catalysis, Siberian Branch of the Russian Academy of Sciences, 630090 Novosibirsk, Russian Federation. Fax: +7 383 333 1617; e-mail: kozlova@catalysis.ru

DOI: 10.1016/j.mencom.2020.03.021

Photocatalysts based on titania and solid solutions of cadmium and zinc sulfides with deposited metals (Pt, Ag) were compared in CO_2 reduction under visible light. In the presence of titania- and cadmium sulfide-based photocatalysts, the dominant reduction products were CH_4 and CO, respectively, due to different positions of the conduction band level for these semiconductors. The deposition of metals on the surface of both TiO_2- and CdS-based samples increased the molar concentration of methane in the reaction products.

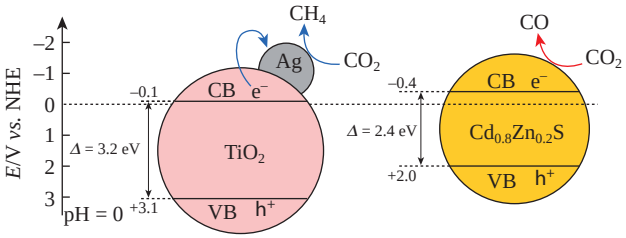

Keywords: cadmium and zinc sulfide solid solution, titanium dioxide, photocatalytic carbon dioxide reduction, visible light.

The rapid exhaustion of easily accessible high-quality natural hydrocarbon feedstock (oil, gas and coal) makes it necessary to harness available alternative energy sources . In the case of solar energy conversion into chemical energy, a remarkable process is the photocatalytic reduction of CO_2, which intrinsically imitates natural photosynthesis in plants. Commercialization of photocatalytic CO_2 reduction is hindered by the absence of efficient heterogeneous photocatalysts.

A search for active heterogeneous photocatalysts for carbon dioxide reduction started in 1989 after publications on the photocatalytic reduction of carbon dioxide in suspensions of semiconductor photocatalysts (TiO_2, CdS, WO_3, ZnO, *etc.*).[1,2] Titania is the most common photocatalyst for CO_2 reduction due to its stability, relatively low price, availability and low toxicity.[3,4] The wide application of TiO_2 is limited by its insensitivity to visible light, which is caused by a large band gap width of 3.2 eV.[5] Efficient titania-based photocatalysts for carbon dioxide reduction are produced by the deposition of various metals.[6,7] Another way to develop such photocatalysts is the synthesis of materials based on semiconductors with narrower band gaps. Metal sulfides (*e.g.*, CdS) attracted attention as CO_2 reduction photocatalysts owing to their appropriate band gaps and catalytic functions.[8] The $Cd_{1-x}Zn_xS$ solid solutions with controllable band gaps and band edge positions are efficient photocatalysts for gas-phase CO_2 reduction under visible light.[9]

The samples based on titanium dioxide[10] or sulfide-based photocatalysts were examined earlier.[8] In this study, photocatalysts based on titania and solid solutions of cadmium and zinc sulfides with deposited metals (Ag, Pt) were compared in the reduction of carbon dioxide under visible light under identical conditions.

Table 1 summarizes the properties of photocatalysts used in this study. The $Cd_{1-x}Zn_xS$ (CZS) photocatalysts were synthesized in accordance with a published procedure.[11] A cadmium to zinc ratio of 2 : 8 was chosen according to our previous results.[9] Metals were deposited on the surface of commercial titania P25 (Evonik Ind., Germany). Silver (1 wt%) was deposited on the titania surface by thermal decomposition of silver nitrate at 120 °C (1% Ag/P25 $AgNO_3$) and its reduction by a twofold excess of $NaBH_4$ (1% Ag/P25 $NaBH_4$); in the case of platinum (1 wt%), photodeposition (1% Pt/P25 photo) and reduction by sodium borohydride (1% Pt/P25 $NaBH_4$) were employed. Platinum and silver were also deposited on the surface of CZS by chemical

Table 1 Properties and activity of photocatalysts for carbon dioxide reduction (285 mW cm^{-2}, 1 atm CO_2 with saturated water vapor, 25 °C).

Entry	Sample	Phase composition	Co-catalyst	$S_{BET}/m^2\ g^{-1}$	$W/\mu mol\ g^{-1}\ h^{-1}$			$R(CO_2)$
					CH_4	CO	H_2	
1	Evonik P25	Anatase/rutile	–	55	0.07	0.85	0.05	2.3
2	1% Pt/P25 photo	Anatase/rutile	Pt^{2+}	55	0.06	0	0	0.5
3	1% Pt/P25 $NaBH_4$	Anatase/rutile	Pt^0	55	0.32	0	0	2.6
4	1% Ag/P25 $AgNO_3$	Anatase/rutile	Ag^0; Ag^+	55	0.59	0	0.10	4.7
5	1% Ag/P25 $NaBH_4$	Anatase/rutile	Ag^0; Ag^+	55	0.58	0	0.13	4.6
6	CZS[9]	$Cd_{0.91}Zn_{0.09}S/Cd_{0.20}Zn_{0.80}S$	–	119	0.22	2.9	0.18	7.6
7	1% Pt/CZS $NaBH_4$	$Cd_{0.91}Zn_{0.09}S/Cd_{0.20}Zn_{0.80}S$	Pt^0; Pt^{2+}	119	0.24	0.53	0.03	2.9
8	1% Ag/CZS $NaBH_4$	$Cd_{0.91}Zn_{0.09}S/Cd_{0.20}Zn_{0.80}S$	Ag^0; Ag^+	119	0.22	0.90	0.17	3.6

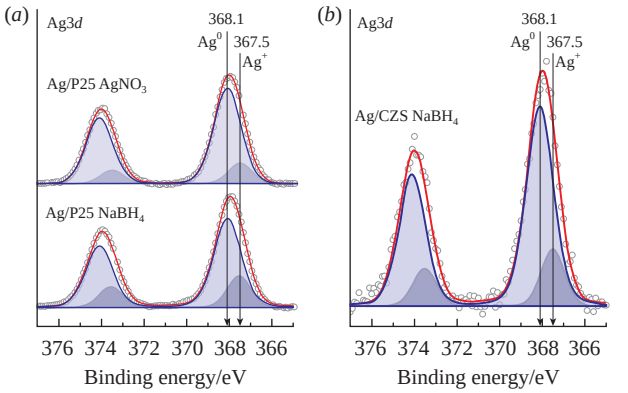

Figure 1 Ag3*d* XPS spectra of (*a*) 1% Ag/P25 $AgNO_3$ and 1% Ag/P25 $NaBH_4$ samples *vs.* (*b*) 1% Ag/CZS $NaBH_4$ sample.

reduction (1% Pt/CZS $NaBH_4$ and 1% Ag/CZS $NaBH_4$ samples). The above methods were successfully used in the synthesis of photocatalysts for the oxidation of harmful organic substances and the production of hydrogen.[12,13] The photocatalysts were examined by XRD, XPS and UV-VIS spectroscopy.

Earlier, it was shown that the CZS photocatalyst with a cadmium to zinc ratio of 8 : 2 consists of two phases, *viz.* $Cd_{0.91}Zn_{0.09}S$ and $Cd_{0.20}Zn_{0.80}S$,† and has a specific surface area of about 120 $m^2\ g^{-1}$.[9] P25 Evonik titania also comprises two phases of anatase and rutile† and has a relatively low specific surface area of 55 $m^2\ g^{-1}$.

We obtained and compared the Pt4*f* spectra of 1% Pt/P25 $NaBH_4$ and 1% Pt/CZS $NaBH_4$ samples:† for the titania-based sample only one doublet with a Pt4$f_{7/2}$ binding energy of 71.1 eV was observed, whereas the spectrum of the CZS sample was approximated by two Pt4$f_{7/2}$–Pt4$f_{5/2}$ doublets with Pt4$f_{7/2}$ binding energies of about 71.1 and 72.2 eV. Thus, platinum on the surface of 1% Pt/CZS $NaBH_4$ occurs in metallic and oxidized states; for the 1% Pt/P25 $NaBH_4$ sample, the reduction by $NaBH_4$ resulted in metallic platinum (see Table 1). The photodeposition of platinum on TiO_2 P25 surface leads to the formation of Pt^{2+} (see Table 1).[13] An analysis of the Ag3*d* XPS spectra (Figure 1) of 1% Ag/P25 $AgNO_3$, 1% Ag/P25 $NaBH_4$, and 1% Ag/CZS $NaBH_4$ samples showed that silver on the surface occurs in two states. The spectra contain peaks with an Ag3$d_{5/2}$ binding energy of 368.1 eV, which is typical of metallic Ag, and a state with E_b(Ag3$d_{5/2}$) = 367.5 eV, which is commonly assigned to silver in Ag_2O oxide.[14] The contribution of the Ag_2O state (E_b = 367.5 eV) to the total intensity of Ag3*d* lines is 15–20% for TiO_2- and CZS-based photocatalysts.

To study the optical properties of photocatalysts, we recorded diffuse reflectance spectra (Figure 2). The absorption edge of the TiO_2 P25 photocatalyst is near 390–400 nm. Weak absorption in the visible region is attributed to the presence of rutile in this sample. The deposition of platinum and silver metals considerably increased absorption in the visible region. For 1% Ag/P25 $AgNO_3$ and 1% Ag/P25 $NaBH_4$ photocatalysts, a diffuse reflectance (R) minimum at ~500 nm was observed due to a plasmon resonance band.[15] For platinum, the plasmon resonance band was observed at 365 nm. Thus, the SPR of Pt nanoparticles sometimes overlapped with that of TiO_2.[16] The CZS photocatalyst has the absorption edge near 500 nm, which is typical of the $Cd_{1-x}Zn_xS$ solid solution with a Cd to Zn ratio of 8 : 2.[11] Deposition of silver or platinum on the CZS surface increased absorption at 500–800 nm.

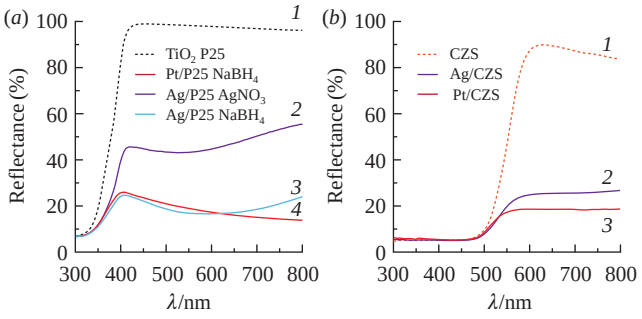

Figure 2 Diffuse reflectance spectra of photocatalysts for carbon dioxide reduction. (*a*): (*1*) TiO_2 P25, (*2*) Ag/P25 $AgNO_3$, (*3*) Ag/P25 $NaBH_4$, (*4*) Pt/P25 $NaBH_4$ and (*b*): (*1*) CZS, (*2*) Ag/CZS, (*3*) Pt/CZS.

† For details, see Online Supplementary Materials.

The experiments on the photocatalytic gas-phase CO_2 conversion with H_2O using samples 1–7 (see Table 1) were performed in a batch mode under irradiation with a 450-nm light-emitting diode (LED) as described earlier.[9] Carbon monoxide, methane and hydrogen were identified as the reduction products of carbon dioxide and water [Figures 3(*a*)–(*c*) and Table 1].

The total rate of carbon dioxide reduction (see Table 1) was calculated from the formula

$$R(CO_2) = [8n(CH_4) + 2n(CO)]/(t\ m), \quad (I)$$

where $n(CH_4)$ and $n(CO)$ are the amounts of formed methane and carbon dioxide, respectively, t is the reaction time, and m is the catalyst weight (g).

The maximum total rate of CO_2 reduction was observed for bare $Cd_{1-x}Zn_xS$ solid solution. Its high activity in comparison with titania-based photocatalysts can be caused by a better absorption in the visible range. Figure 2 and Table 3 indicate that, in the presence of unmodified titania, the main product is CO, whereas CH_4 was the main product upon the deposition of metals on TiO_2. In the case of the CZS sample, the deposition of silver or platinum increased the molar concentration of methane from 9 to 16–28% (see Figure 3).

It is well known that the following reactions occur during the photocatalytic reduction of CO_2 with H_2O.[17]

$$CO_2 + 2H^+ + 2e^- \rightarrow CO + H_2O \qquad E^0 = -0.12\ V \text{ at pH } 0 \quad (1)$$

$$CO_2 + 8H^+ + 8e^- \rightarrow CH_4 + 2H_2O \qquad E^0 = 0.17\ V \text{ at pH } 0 \quad (2)$$

The CB potential of CZS ($Cd_{0.91}Zn_{0.09}S/Cd_{0.20}Zn_{0.80}S$) lies at –0.4 V *vs.* NHE at pH 0, whereas the CB potential of TiO_2 is –0.1 V *vs.* NHE at pH 0.[18] Thus, the CB potential of CZS is more negative than the reduction potential $E^0_{CO_2/CO}$ (–0.12 V), while these potentials for TiO_2 are almost the same; thus, both processes are theoretically possible. Although the reduction potentials $E^0_{CO_2/CH_4}$ are less negative than $E^0_{CO_2/CO}$, eight electrons are required to produce CH_4 and only two, to produce CO. The samples with deposited metals increase the efficiency of many-electron process of CH_4 formation, whereas the formation of CO is suppressed. The enriched electron density near the surface of metal nanoparticles favored the reduction of CO_2 to CH_4, as the formation of CH_4 is thermodynamically more feasible than the formation of CO if the quantity of excited electrons is sufficient.[10]

Note that the deposition of Ag/Ag_2O (1% Ag/P25 $AgNO_3$ and 1% Ag/P25 $NaBH_4$) co-catalysts on the surface of TiO_2 leads to an increase in the activity of CO_2 reduction, whereas the deposition of platinum (1% Pt/P25 $NaBH_4$) only changes the distribution of products. A higher activity of the samples with deposited silver under visible light is related to the presence of SPR absorption of Ag nanoparticles in the visible region. Moreover, the high activity of Ag/Ag_2O/TiO_2 composite photocatalysts can also be explained by the formation of heterojunctions in a ternary system.[19,20] Interestingly, the deposition of metals on a CZS solid solution of cadmium and zinc sulfides reduces photocatalytic activity. Unlike titanium dioxide, the solid solution has a high absorption

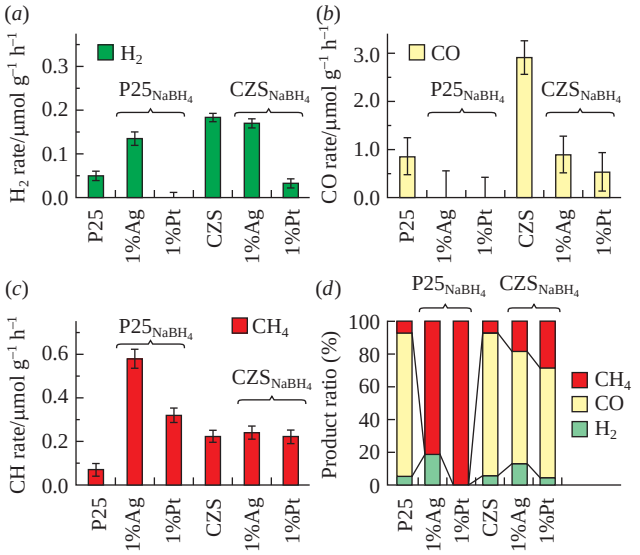

Figure 3 Rates of formation of (*a*) hydrogen, (*b*) carbon monoxide and (*c*) methane over the samples; (*d*) distribution of carbon dioxide and water reduction products over the photocatalysts. Conditions: 285 mW cm^2, 1 atm CO_2 with saturated water vapor, 25 °C.

in the visible region. Metal particles can act as recombination centres to reduce the rate of the target process.[21]

The titania-based catalysts are more efficient in the formation of methane, whereas those based on cadmium and zinc sulfides, even 1% Pt/CZS $NaBH_4$ and 1% Ag/CZS $NaBH_4$ samples, in the formation of CO. The distribution of products depends on the conduction band level of the semiconductor photocatalyst.[9] As described above, the CB potential of CZS (–0.4 V *vs.* NHE) is higher that that of TiO_2 (–0.1 V *vs.* NHE).[18] Thus, carbon dioxide reduction with the formation of carbon monoxide proceeds more efficiently over the photocatalyst based on cadmium and zinc sulfides.

The rate of carbon monoxide formation over CZS was high as compared to published data on CO_2 reduction over $Cd_{1-x}Zn_xS$-based photocatalysts,[8] and the rate of methane formation in the presence of TiO_2-based samples is comparable with published data.[16]

Thus, we found that, under similar conditions, the dominant reduction product in the presence of titania-based samples was CH_4, while CO was the dominant product in the case of photocatalysts based on cadmium sulfide due to different conduction band levels of TiO_2 and $Cd_{1-x}Zn_xS$. To provide a sufficient activity, the deposition of a metallic co-catalyst on the titania surface is required, whereas sulfide photocatalysts can operate in an unmodified state. The deposition of metals on the surfaces of both TiO_2- and CdS-based samples increased the molar concentration of methane in the reaction products.

This work was supported by the Ministry of Science and Higher Education of the Russian Federation (project no. AAA-A17-117041710087-3) and the Russian Foundation for Basic Research (grant no. 18-03-00775).

Online Supplementary Materials

Supplementary data associated with this article can be found in the online version at doi: 10.1016/j.mencom.2020.03.021.

References

1 T. Inoue, A. Fujishima, S. Konishi and K. Honda, *Nature*, 1979, **277**, 637.
2 A. A. Ulyankina, A. B. Kuriganova and N. V. Smirnova, *Mendeleev Commun.*, 2019, **29**, 215.
3 I. A. Kovalev, A. A. Petrov, O. A. Ibragimova, A. V. Shokod'ko, A. S. Chernyavskii, E. A. Goodilin, K. A. Solntsev and A. B. Tarasov, *Mendeleev Commun.*, 2018, **28**, 541.
4 M. V. Korolenko, P. B. Fabritchnyi, M. I. Afanasov and C. Labrugère, *Mendeleev Commun.*, 2019, **29**, 718.
5 A. Corma and H. Garcia, *J. Catal.*, 2013, **308**, 168.
6 H. G. Badoví, Ş. Neatu, A. Khan, A. M. Asiri, S. A. Kosa and H. Garcia, *J. Phys. Chem. C*, 2015, **119**, 6819.
7 T. Zhang, J. Low, X. Huang, J. F. AI-Sharab, J. Yu and T. Asefa, *ChemCatChem*, 2017, **9**, 3054.
8 X. Meng, G. Zuo, P. Zong, H. Pang, J. Ren, X. Zeng, S. Liu, Y. Shen, W. Zhou and J. Ye, *Appl. Catal., B*, 2018, **237**, 68.
9 E. A. Kozlova, M. N. Lyulyukin, D. V. Markovskaya, D. S. Selishchev, S. V. Cherepanova and D. V. Kozlov, *Photochem. Photobiol. Sci.*, 2019, **18**, 871.
10 K.-Y. Lee, K. Sato and A. R. Mohamed, *Mater. Lett.*, 2016, **163**, 240.
11 T. P. Lyubina and E. A. Kozlova, *Kinet. Catal.*, 2012, **53**, 188 (*Kinet. Katal.*, 2012, **53**, 197).
12 P. A. Kolinko, D. S. Selishchev and D. V. Kozlov, *Theor. Exp. Chem.*, 2015, **51**, 96 (*Teor. Eksp. Khim.*, 2015, **51**, 88).
13 E. A. Kozlova, T. P. Lyubina, M. A. Nasalevich, A. V. Vorontsov, A. V. Miller, V. V. Kaichev and V. N. Parmon, *Catal. Commun.*, 2011, **12**, 597.
14 V. I. Bukhtiyarov, M. Hävecker, V. V. Kaichev, A. Knop-Gericke, R. W. Mayer and R. Schlögl, *Phys. Rev. B*, 2003, **67**, 235422.
15 E. Liu, L. Kang, F. Wu, T. Sun, X. Hu, Y. Yang, H. Liu and J. Fan, *Plasmonics*, 2014, **9**, 61.
16 Y. Ma and Z. Li, *Appl. Surf. Sci.*, 2019, **493**, 1142.
17 S. N. Habisreutinger, L. Schmidt-Mende and J. K. Stolarczyk, *Angew. Chem., Int. Ed.*, 2013, **52**, 7372.
18 D. Jing, L. Guo, L. Zhao, X. Zhang, H. Liu, M. Li, S. Shen, G. Liu, X. Hu, X. Zhang., K. Zhang, L. Ma and P. Guo, *Int. J. Hydrogen Energy*, 2010, **35**, 7087.
19 R. El-Shabasy, N. Yosri, H. El-Seedi, K. Shoueir and M. El-Kemary, *Optik*, 2010, **192**, 162943.
20 H. Xu, J. Xie, W. Jia, G. Wu and Y. Cao, *J. Colloid Interface Sci.*, 2018, **516**, 511.
21 E. A. Kozlova and V. N. Parmon, *Russ. Chem. Rev.*, 2017, **86**, 870.

Received: 29th August 2019; Com. 19/6020